Analysis of synchronous machine modeling for simulation and industrial applications

Abdallah Barakat [a,b,*], Slim Tnani [a], Gérard Champenois [a], Emile Mouni [b]

[a] University of Poitiers, Laboratoire d'Automatique et d'Informatique Industrielle, Bâtiment mécanique, 40 avenue du Recteur Pineau, 86022 Poitiers, France
[b] Leroy-Somer Motors, Bd Marcellin Leroy, 16015 Angoulême, France

ARTICLE INFO

ABSTRACT

This paper analyses the synchronous machine modeling by taken into account the machine parameters usually used in industry and those used in researcher's domains. Two models are presented. The first one is developed in the (d, q) natural reference frames and the other one is referred to the (d, q) stator reference frame. To do this, two methods are proposed to compute the reduction factor of the field winding without any input from design information. It is shown that the reduction factors of the (d, q) damper windings do not influence on the terminal behavior of the machine. This means that it is possible to know the terminal behavior of the machine without knowing the real inductances and resistances of the damper windings. The accuracy of these models is validated by experimental tests.

1. Introduction

Synchronous machines are used in many fields, as in motor applications or in generator applications. The goals to have a synchronous machine model can be split into two groups: (1) to achieve further insight in the complex electro-magnetic behavior of the machine [1,2] and (2) for simulation or control purposes [3].

By using finite element methods (FEMs), it became possible to have a very accurate electro-magnetic description of the machine, but the two main problems are the computation time in FEM simulations and the large number of parameters of the electrical machine [4,5]. For this reason, FEM are very useful to achieve insight during the design stage of the machine.

Synchronous machine is also used in power generation [6,7]. In most cases, the synchronous generator is excited by a diode bridge rectifier connected to the three-phase stator of an excitation machine. The control of the terminal voltage of the main machine requires the modeling of the main machine, the diode bridge and the excitation machine. In this application, a linear model which represents the dynamic behavior of the system permits to synthesize a linear robust controller by using the advanced theory of control system [6]. The real-time implementation of control applications in a calculator such as a Microcontroller or FPGA requires non-complex tasks to reduce the computational effort and the execution time [8]. A linear model is very useful to synthesize a linear controller. This paper presents a linear model for synchronous machine with damper windings.

Recently, the author in [9] has identified the Park model parameters by using an equivalent circuit for the machine. This circuit includes the stator windings and the rotor windings without using the same magnetic circuit. For this reason, the mutual inductance between the d-axis stator winding and the d-axis damper winding will be equal to the mutual inductance between the d-axis stator winding and the main field winding. By referring the rotor parameters to the stator frame, authors
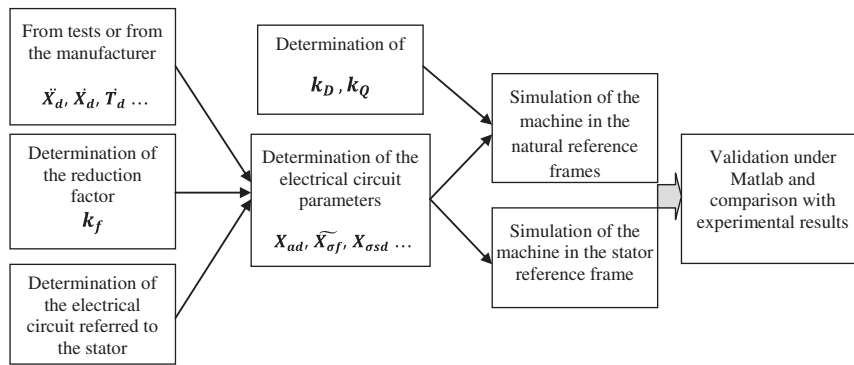

Fig. 1. Block diagram of the work organization.

in [10,11] have used an equivalent circuit which includes the stator and the rotor windings in the same magnetic circuit. This method is more general than the first one, but the determination of the reduction coefficients used to refer the rotor winding to the stator frame depends on the design information of the machine [10,12]. The author in [10] has used a simple correction factor; the author in [13] has used the finite element model to compute these coefficients.

Present work has been carried out in five sections. After the introduction given in Section 1, the modeling of the machine is presented in Section 2. From the classical machine equations, the mathematical model is found in the (d,q) natural reference frames. The fluxes partition is used to find an equivalent circuit where the machine parameters are referred to the (d,q) stator reference frame. The main field winding, the d-axis damper winding, and the q-axis damper winding are referred to the stator frame. To do this, three reduction factors are used: k_f, k_D, k_Q. The machine model presented in the stator reference frame proves that the values of k_D and k_q do not affect the terminal behavior of the machine. In Section 3, we have determined the relationships between the machine parameters in the natural reference frames and those used in the stator reference frame. The relationships between the parameters usually given by the manufacturer and those used in modeling are also given. Without any input from design information, two methods are proposed to compute the reduction factor of the main field winding (k_f). These methods are compared with those found in the literatures. In Section 4, an experimental test bench is presented. From the parameters given by the manufacturer and by making a short-circuit test, the machine parameters are determined. The implementation under Matlab/Simulink is provided by using the concept of state equations. In Section 5, a comparison between practical tests and the corresponding numerical results is done. A sudden short-circuit test and a sudden open-circuit test are done. The both tests are used to identify the synchronous machine, but the first one is very interesting to excite the damper windings. A discussion on the sources of the encountered discrepancies and interpretation of the modeling improvement are also presented. Fig. 1 resumes the work organization in this paper.

2. Synchronous machine modeling

For synchronous machine studies, the two axis equivalent circuits with two or three damping windings are usually assumed at the proper structures [14]. In this paper, and using Park transformation, the synchronous machine is supposed to be modeled with one damper winding for the d-axis and a one damper winding for the q-axis.

2.1. Voltage and flux equations in the natural reference frames

In developing the basic equations of a synchronous machine, the following assumptions are made:

- The stator windings are symmetrical and have a perfect sinusoidal distribution along the air gap.
- The permeance of the magnetic paths on the rotor is independent of the rotor positions.
- Saturation and hysteresis effects are inexistent.

Fig. 2 shows a representation of a synchronous machine. By adopting generator convention for the stator windings, voltage equations can be written as follows:

$$V_{abc} = -r_s I_{abc} + \frac{d}{dt}\Phi_{abc} \quad v_f = r_f i_f + \frac{d}{dt}\varphi_f$$

$$0 = r_D i_D + \frac{d}{dt}\varphi_D \quad 0 = r_Q i_Q + \frac{d}{dt}\varphi_Q \tag{1}$$

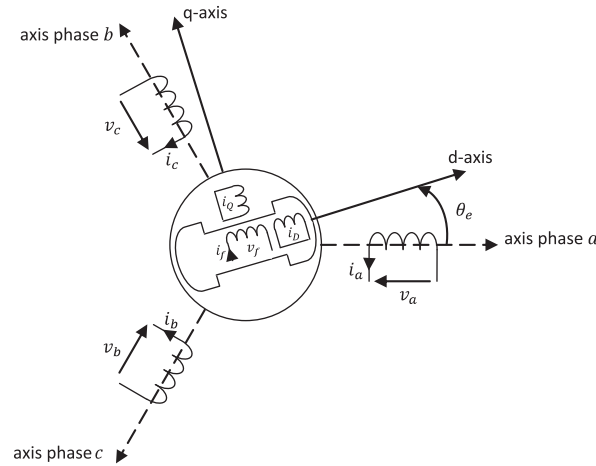**Fig. 2.** Wound rotor synchronous machine with dampers.

where:

- i_D, i_Q: direct and transverse dampers currents.
- φ_D, φ_Q: direct and transverse dampers total flux.
- Φ_{abc}: stator total flux, φ_f: main field total flux.
- r_s: stator resistance, r_f: main field resistance, r_D and r_Q: dampers resistances.
- V_{abc}, I_{abc}: output voltages and armature currents, respectively.
- v_f, i_f: main field excitation voltage and main field current, respectively.

2.2. Voltage and flux equation in the dq frame

By using Park's transformation defined by Eq. (2) according to the machine's electrical angle θ_e, stator quantities will be projected on the rotating d-axis and q-axis. The rotor windings are not subject to any transformation at all because they are oriented in the d-axis and q-axis by assumption.

$$P(\theta_e) = \frac{\sqrt{2}}{\sqrt{3}} \begin{bmatrix} \cos(\theta_e) & \cos\left(\theta_e - \frac{2\pi}{3}\right) & \cos\left(\theta_e + \frac{2\pi}{3}\right) \\ -\sin(\theta_e) & -\sin\left(\theta_e - \frac{2\pi}{3}\right) & -\sin\left(\theta_e + \frac{2\pi}{3}\right) \end{bmatrix} \tag{2}$$

By applying the transformation matrix such as: $v_{dq} = P(\theta_e)V_{abc}$ and $\varphi_{dq} = P(\theta_e)\varphi_{abc}$, the voltage and flux linkage equations are given by [9]:

$$
\begin{aligned}
&\text{Flux linkage equations :} && \text{Voltage equations :} \\
&\varphi_d = -L_d i_d + m_{sf} i_f + m_{sD} i_D && v_d = -r_s i_d - \omega_e \varphi_q + \frac{d\varphi_d}{dt} \\
&\varphi_q = -L_q i_q + m_{sQ} i_Q && v_q = -r_s i_q + \omega_e \varphi_d + \frac{d\varphi_q}{dt} \\
&\varphi_f = L_f i_f + m_{fD} i_D - m_{sf} i_d && v_f = r_f i_f + \frac{d\varphi_f}{dt} \\
&\varphi_D = L_D i_D + m_{fD} i_f - m_{sD} i_d && 0 = r_D i_D + \frac{d\varphi_D}{dt} \\
&\varphi_Q = L_Q i_Q - m_{sQ} i_q && 0 = r_Q i_Q + \frac{d\varphi_Q}{dt}
\end{aligned}
\tag{3}
$$

where:

- L_D, L_Q: inductances of the direct and quadrature damper windings.
- L_f: inductance of the main field winding.
- L_d, L_q: inductances of the d-axis stator winding and q-axis stator winding.
- m_{sf}: mutual inductance between the field winding and the d-axis stator winding.
- m_{sD}: mutual inductance between the d-axis stator winding and the d-axis damper winding.
- m_{sQ}: mutual inductance between the q-axis stator winding and the q-axis damper winding.
- m_{fD}: mutual inductance between the field winding and the d-axis damper winding.

2.3. Machine modeling in the stator reference frame

On the one hand, the simulation of the machine model presented by Eq. (3) requires the determination of the machine parameters in the natural reference frames: $m_{sD}, m_{sf}, m_{fD}, L_D, \ldots$. On the other hand, the manufacturer or practical tests do not determine directly the above parameters [15,16]. They determine reactances and time constants of the machine such as the direct axis transient reactance and the direct axis subtransient reactance.... The relationship between the quantities given by the manufacturer and the required parameters in Eq. (3) is determined by using an equivalent circuit of the machine [17]. By referring the rotor quantities to the stator side, the equivalent circuit will be found.

2.3.1. Voltage and flux equations referred to the stator frame

To refer the rotor parameters to the stator side, k_f is defined as the reduction factor between the main field winding and the d-axis stator winding, k_D the reduction factor between the d-axis damper winding and the d-axis stator winding, the reduction factor between the k_Q q-axis damper winding and the q-axis stator winding: $\tilde{i}_f = \frac{i_f}{k_f}$, $\tilde{i}_D = \frac{i_D}{k_D}$, $\tilde{i}_Q = \frac{i_Q}{k_Q}$, $\widetilde{\varphi}_f = k_f \varphi_f$, $\widetilde{\varphi}_D = k_D \varphi_D$, $\widetilde{\varphi}_Q = k_Q \varphi_Q$, $\widetilde{v}_f = k_f v_f$, $\tilde{i}_f$, $\tilde{i}_D$ and $\tilde{i}_Q$ are the referred currents to the stator side. By using these coefficients (k_f, k_D, k_Q), Eq. (3) is rewritten by referring all variables to the stator frame:

$$
\begin{aligned}
&\text{Flux linkage equations :} && \text{Voltage equations :} \\
&\varphi_d = -L_d i_d + m_{sf} k_f \tilde{i}_f + m_{sD} k_D \tilde{i}_D && v_d = -r_s i_d - \omega_e \varphi_q + \frac{d\varphi_d}{dt} \\
&\varphi_q = -L_q i_q + m_{sQ} k_Q \tilde{i}_Q && v_q = -r_s i_q + \omega_e \varphi_d + \frac{d\varphi_q}{dt} \\
&\widetilde{\varphi}_f / k_f = L_f k_f \tilde{i}_f + m_{fD} k_D \tilde{i}_D - m_{sf} i_d && \frac{\widetilde{v}_f}{k_f} = r_f k_f \tilde{i}_f + \frac{1}{k_f} \frac{d\widetilde{\varphi}_f}{dt} \quad \text{or} \quad \widetilde{v}_f = \widetilde{r}_f \tilde{i}_f + \frac{d\widetilde{\varphi}_f}{dt} \\
&\widetilde{\varphi}_D / k_D = L_D k_D \tilde{i}_D + m_{fD} k_f \tilde{i}_f - m_{sD} i_d && 0 = \widetilde{r}_D \tilde{i}_D + \frac{d\widetilde{\varphi}_D}{dt} \\
&\widetilde{\varphi}_Q / k_Q = L_Q k_Q \tilde{i}_Q - m_{sQ} i_q && 0 = \widetilde{r}_Q \tilde{i}_Q + \frac{d\widetilde{\varphi}_Q}{dt} \\
& && \text{where :} \quad r_f = \frac{\widetilde{r}_f}{k_f^2} \quad r_D = \frac{\widetilde{r}_D}{k_D^2} \quad r_Q = \frac{\widetilde{r}_Q}{k_Q^2}
\end{aligned}
\tag{4}
$$

2.3.2. Determination of the equivalent circuit in the stator frame

Fig. 3 clearly shows the interaction between the stator fluxes and the rotor fluxes. This figure serves to find the electrical circuit of the machine. We have assumed that any winding is not influenced by the leakage flux of another winding [13,18]. For example, the main field winding is not influenced by the leakage flux $\varphi_{\sigma sd}$ and $\widetilde{\varphi}_{\sigma D}$. In this figure, all variables are referred to the stator.

- d-axis:
  - $\widetilde{\varphi}_{\sigma D}$: the direct damper leakage flux referred to the stator.
  - $\widetilde{\varphi}_{\sigma f}$: the main field leakage flux referred to the stator.
  - $\varphi_{\sigma sd}$: the leakage flux of the d-axis stator winding.
  - φ_{ad}: the direct main flux.
- q-axis:
  - $\widetilde{\varphi}_{\sigma Q}$: the transverse damper leakage flux referred to the stator.
  - $\varphi_{\sigma sq}$: the q-axis stator winding leakage flux.
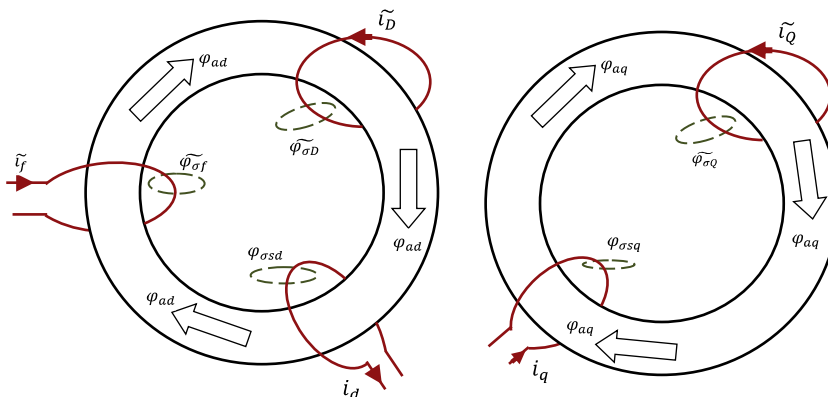 - φ_{aq}: the transverse main flux.

Fig. 3. Interaction between rotor fluxes and stator fluxes.

From Fig. 3, fluxes repartition can be described by Eq. (5):

$$
\begin{aligned}
\varphi_d &= \varphi_{ad} + \varphi_{\sigma sd} = L_{ad}\left(-i_d + \widetilde{i_D} + \widetilde{i_f}\right) - L_{\sigma sd}i_d \\
\varphi_q &= \varphi_{aq} + \varphi_{\sigma sq} = L_{aq}\left(-i_q + \widetilde{i_Q}\right) - L_{\sigma sq}i_q \\
\widetilde{\varphi_f} &= \varphi_{ad} + \widetilde{\varphi_{\sigma f}} = L_{ad}\left(-i_d + \widetilde{i_D} + \widetilde{i_f}\right) + \widetilde{L_{\sigma f}}\,\widetilde{i_f} \\
\widetilde{\varphi_D} &= \varphi_{ad} + \widetilde{\varphi_{\sigma D}} = L_{ad}\left(-i_d + \widetilde{i_D} + \widetilde{i_f}\right) + \widetilde{L_{\sigma D}}\,\widetilde{i_D} \\
\widetilde{\varphi_Q} &= \varphi_{ad} + \widetilde{\varphi_{\sigma Q}} = L_{ad}\left(-i_q + \widetilde{i_Q}\right) + \widetilde{L_{\sigma Q}}\,\widetilde{i_Q}
\end{aligned}
\tag{5}
$$

where:

- $L_{\sigma sd}$ and $L_{\sigma sq}$ are direct and transverse stator leakage inductances.
- $\widetilde{L_{\sigma f}}$ is the main field leakage inductance referred to the stator.
- L_{ad} and L_{aq} are direct and transverse stator main inductances.
- $\widetilde{L_{\sigma D}}$ and $\widetilde{L_{\sigma Q}}$ are dampers leakage inductances referred to the stator.

By using the machine voltage equations (Eq. (4)) and the flux linkage equations (Eq. (5)), the electrical circuit of the machine can be deduced as follows:

The above equivalent circuit can be used to simulate the synchronous machine behavior. From Figs. 4 and 5, it is possible to simulate the machine behavior and measure the terminal voltage and the terminal current without using the reduction factors k_D and k_Q. k_f is used to compute the referred voltage $\widetilde{v_f}$ from the real voltage v_f.

3. Relationships between the machine parameters

3.1. Determination of the machine parameters in the natural frames

The first machine model is presented in the natural frames; the second one is developed in the stator reference frame. By comparing Eq. (4) with Eq. (5), the machine parameters in the natural frames can be deduced as follows:

$$
\begin{aligned}
&L_d = L_{ad} + L_{\sigma sd} \quad L_q = L_{aq} + L_{\sigma sq} \\
&m_{sQ} = \frac{L_{aq}}{k_Q} \quad m_{sf} = \frac{L_{ad}}{k_f} \quad m_{sD} = \frac{L_{ad}}{k_D} \quad m_{fD} = \frac{L_{ad}}{k_f k_D} \\
&L_f = \frac{L_{ad}}{k_f^2} + \frac{\widetilde{L_{\sigma f}}}{k_f^2} \quad L_D = \frac{L_{ad}}{k_D^2} + \frac{\widetilde{L_{\sigma D}}}{k_D^2} \quad L_Q = \frac{L_{ad}}{k_Q^2} + \frac{\widetilde{L_{\sigma Q}}}{k_Q^2} \\
&r_f = \frac{\widetilde{r_f}}{k_f^2} \quad r_D = \frac{\widetilde{r_D}}{k_D^2} \quad r_Q = \frac{\widetilde{r_Q}}{k_Q^2}
\end{aligned}
\tag{6}
$$

As shown in Eq. (6), the determination of the machine parameters in the natural reference frame requires the determination of the electrical circuit parameters (see Fig. 3) such as $\widetilde{L_{\sigma f}}, \widetilde{L_{\sigma D}}, \widetilde{L_{\sigma Q}}, \widetilde{r_D} \ldots$ These parameters will be computed from the quantities given by the manufacturer or by identification tests.

Table 1 shows some reactances and time constants of a synchronous machine. These parameters are given by the manufacturer or by identification tests [9].

According to the IEEE and IEC standards [15], the relationship between parameters given in Table 1 and those given in Fig. 4 can be written as follows:
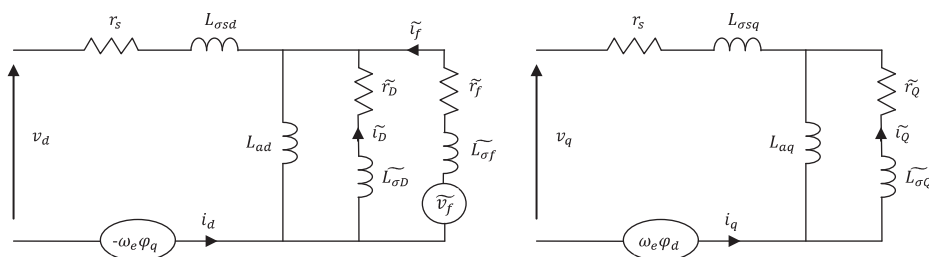

Fig. 4. Electrical circuit by referring the rotor quantities to the stator side.

Table 1
Machine parameters given by the manufacturer.

Reactances and time constants	
X_d	Direct axis synchronous reactance unsaturated
X_q	Quadrature axis synchronous reactance unsaturated
$\dot{T}_{do}$	Direct axis open-circuit time constant
$\dot{X}_d$	Direct axis transient reactance saturated
$\dot{T}_d$	Short-circuit transient time constant
$\ddot{X}_d$	Direct axis subtransient reactance saturated
$\ddot{T}_d$	Direct axis subtransient time constant
$\ddot{X}_q$	Quadrature axis subtransient reactance saturated

- $X = L\omega_e$
- $X_d = X_{\sigma sd} + X_{ad}$ $\dot{X}_d = X_{\sigma sd} + \frac{X_{ad}\widetilde{X_{\sigma f}}}{X_{ad}+X_{\sigma f}}$ $\ddot{X}_d = X_{\sigma sd} + \frac{\widetilde{X_{\sigma D}}\widetilde{X_{\sigma f}}}{X_{\sigma D}+X_{\sigma f}}$
- $X_q = X_{\sigma sq} + X_{aq}$ $\ddot{X}_q = X_{\sigma sq} + \frac{\widetilde{X_{\sigma q}}X_{aq}}{X_{\sigma D}+X_{aq}}$
- $\dot{T}_{do} = \frac{X_{ad}+\widetilde{X_{\sigma f}}}{\omega_e \widetilde{r_f}}$ $\dot{T}_d = \frac{1}{\omega_e \widetilde{r_f}}\left(\widetilde{X_{\sigma f}} + \frac{X_{ad}X_{\sigma sd}}{X_{ad}+X_{\sigma sd}}\right)$
- $\ddot{T}_{do} = \frac{1}{\omega_e \widetilde{r_D}}\left(\widetilde{X_{\sigma D}} + \frac{X_{ad}\widetilde{X_{\sigma f}}}{X_{ad}+X_{\sigma f}}\right)$ $\ddot{T}_d = \frac{1}{\omega_e \widetilde{r_D}}\left(\widetilde{X_{\sigma D}} + \frac{X_{\sigma sd}\widetilde{X_{\sigma f}}}{X_{\sigma sd}+X_{\sigma f}}\right)$
- $\ddot{T}_{qo} = \frac{X_{aq}+\widetilde{X_{\sigma Q}}}{\omega_e \widetilde{r_Q}}$ $\ddot{T}_q = \frac{1}{\omega_e \widetilde{r_Q}}\left(\widetilde{X_{\sigma Q}} + \frac{X_{aq}X_{\sigma sq}}{X_{aq}+X_{\sigma sq}}\right)$

By using the above equations, Table 2 shows the relationship between the parameters presented in Table 1 and those defined in the electrical circuit of the machine [9].

By using the relationships presented in Table 2 and Eq. (2) it will be possible to determine the machine parameters in the natural reference frame. So, the simulation of the model presented by Eq. (3) will be also possible.

As shown in Table 2, the computing of the field winding resistance $(\widetilde{r_f})$, requires the determination of the reduction factor k_f.

3.2. Determination of the reduction factors

3.2.1. Reduction factor of the excitation winding: k_f

The magnetomotrice force (MMF) created by the stator windings has two components: F_d and F_q. In the d-axis, F_d is created by the current i_d. The second component F_q is created by the current i_q. The MMF created by the main field winding is only in the d-axis. The reduction factor k_f is determined by computing the main excitation current i_{excd} that generates the same MMF F_d. In this case:

$$k_f = \frac{i_{excd}}{i_d} \tag{7}$$

The used Park transformation keeps the invariance principle of powers. So, the current i_d presented in Eq. (7) is the measured one in the Park frame. Some methods will be proposed to compute the reduction factor k_f.

1. In [10] the author determines k_f by the following equation:

$$k_f = \frac{\sqrt{3}}{2\sqrt{2}}\frac{N_a}{pN_r}k_a \tag{8}$$

Table 2
Relationships between the manufacturer quantities and the equivalent circuit parameters.

$\frac{\dot{T}_{da}}{\dot{T}_d} = \frac{X_d}{\dot{X}_d}$ $\frac{\ddot{T}_{do}}{\ddot{T}_d} = \frac{\dot{X}_d}{\ddot{X}_d}$ $\frac{\ddot{T}_{qo}}{\ddot{T}_q} = \frac{X_q}{\ddot{X}_q}$	
$X_{ad} = \sqrt{\dot{T}_{do}\omega_e \widetilde{r_f}(X_d - \dot{X}_d)}$	$X_{aq} = \sqrt{\widetilde{r_Q}X_q\omega_e\left(\ddot{T}_{qo} - \ddot{T}_q\right)}$
$X_{\sigma sd} = X_d - X_{ad}$	$\widetilde{X_{\sigma f}} = \dot{T}_{do}\omega_e \widetilde{r_f} - X_{ad}$
$\widetilde{r_D} = \frac{1}{\omega_e\ddot{T}_{do}}\left(\widetilde{X_{\sigma D}} + \frac{X_{ad}\widetilde{X_{\sigma f}}}{X_{\sigma f}+X_{ad}}\right)$	$\widetilde{X_{\sigma D}} = \frac{(\dot{X}_d - X_{\sigma sd})\widetilde{X_{\sigma f}}}{X_{\sigma f}+X_{\sigma sd}-\dot{X}_d}$
$X_{\sigma sq} = X_q - X_{aq}$	$\widetilde{X_{\sigma Q}} = \widetilde{r_Q}\omega_e\ddot{T}_{qo} - X_{aq}$

- N_a: number of turns in series in one phase stator winding.
- N_r: number of turns in one pole of the main field windings.
- p: number of pole pairs.
- k_a: a corrector factor.

2. k_f can be determined by using a finite element model [13]. The author has shown the influence of the excitation current and saturation on k_f value.

3. In [12] k_f is determined by using the following equation:

$$k_f = \frac{\sqrt{6}}{\pi} \frac{N_a}{pN_r} k_b k_c \tag{9}$$

- k_b: a constant which takes into account the winding factor for the fundamental harmonic of the MMF ($k_b \approx 0.9$).
- k_c: This factor is called the coefficient of the longitudinal reaction. It depends on the geometrical data of the machine poles.
  By comparison of Eqs. (8) and (9): $k_a = \frac{4}{\pi} k_b k_c$.

The first method supposes that the MMF of the stator windings and the MMF of the main field winding are sinusoidal. The second method takes into consideration the harmonics. The factor k_c depends on the geometrical data of the machine. k_f is computed from knowledge of the numbers of stator and rotor turns, their distribution and their pitch. This information is not always given by the manufacturer. For this reason, the machine modeling presented in Section 2 will be used to determine the reduction factor k_f:

(1) From Fig. 3, the excitation winding is not changed but the excitation current becomes $\tilde{i}_f$. The mutual inductance between the main field winding and the d-axis stator winding is L_{ad}. In the natural reference frame, the mutual inductance between the main field winding and the d-axis stator winding is m_{sf}. So, the constant k_f is equal to: $\frac{L_{ad}}{m_{sf}}$. Mathematically, this result can be proved by using Eq. (6). In most cases, $L_{\sigma sd} \ll L_{ad}$ and $\widetilde{L_{\sigma f}} \ll L_{ad}$. So, $L_d \approx L_{ad}$ and the following equation can be deduced:

$$\left\{ \begin{array}{l} m_{sf} = \frac{L_{ad}}{k_f} \\ L_f = \frac{L_{ad}}{k_f^2} + \frac{\widetilde{L_{\sigma f}}}{k_f^2} \end{array} \right\} \rightarrow k_f = \frac{L_{ad}}{m_{sf}} \approx \frac{L_d}{m_{sf}} \quad \text{or} \quad k_f \approx \frac{m_{sf}}{L_f} \tag{10}$$

(2) In the steady state of a short-circuit test ($v_d = v_q = 0V$), the stator voltage equations are:

$$\begin{aligned} v_d &= 0 = -r_s i_d + L_q \omega_e i_q \\ v_q &= 0 = -r_s i_q - L_d \omega_e i_d + m_{sf} \omega_e i_f \end{aligned} \tag{11}$$

As known ($l_d \omega_e i_d \gg r_s i_q$), the following equation can be deduced:

$$\begin{aligned} 0 &= -L_d \omega_e i_d + m_{sf} \omega_e i_f \\ &\Downarrow \\ \frac{i_f}{i_d} &= \frac{L_d}{m_{sf}} \end{aligned} \tag{12}$$

By using Eqs. (10) and (11), the reduction factor k_f can be determined as follows:

$$k_f \approx \frac{i_f}{i_d} \approx \frac{i_f}{\sqrt{3} i_{aeff}} \tag{13}$$

The above result explains the definition given at the beginning of this subsection. It also shows the influence of the leakage fluxes. As shown in Eq. (13), the reduction factor of the excitation field winding can be obtained directly from the steady state short-circuit test (short-circuit armature current versus the main field winding current) and without any input from design information.

3.2.2. Reduction factors of the dampers: k_D and k_Q

From Table 2, it is shown that the dampers parameters are computed without the using of k_D and k_Q. From the equivalent circuit of the machine (see Fig. 4) and the mathematical model presented by Eq. (4), it is noticed that is possible to simulate the machine behavior without the using of the reduction factors of the dampers. These factors are essentially used to measure the real values of the currents i_D and i_Q $\left(i_D = k_D \tilde{i}_D, i_Q = k_Q \tilde{i}_Q \right)$. In [13], the author has used the finite element method to determine these factors.

4. Simulation and practical tests

4.1. Experimental test bench presentation

The machine used in this paper is a 75 kV A salient-pole synchronous machine with damper windings. The standard quantities given by the manufacturer (Leroy-Somer Motors) are presented in Table 3. These quantities have been checked by using identification tests [15].

As shown in Fig. 5, the experimental bench is composed by three machines coupled on the same shaft. The test machine is the main synchronous machine. This machine is excited by a diode bridge rectifier connected to the rotating three-phase of an excitation machine. The last one is a synchronous machine which has stationary field coils and a rotating armature. The prime mover is a synchronous motor connected to the main electrical grid.

4.2. Identification of the reductions factors: k_f, k_D, k_Q

The methods listed in Section 3.2 are used: (1) classical tests are used to measure m_{sf} and L_f: m_{sf} = 193.9 mH and L_f = 2.28 H. From Eq. (10), the obtained value of k_f is 0.085; (2) Fig. 6a shows the short-circuit characteristic (short-circuit armature current versus the main field winding current). Fig. 6b illustrates the different values of k_f. These values are computed by using Eq. (13) and the short-circuit test. The obtained mean value of k_f is 0.088. By using the obtained value for k_f (0.088), one can compute the constant of the machine: k_c = 0.7. From [12], this factor depends on the number of pole pairs and the geometrical data of pole windings.

Table 3
Synchronous machine parameters and nominal values.

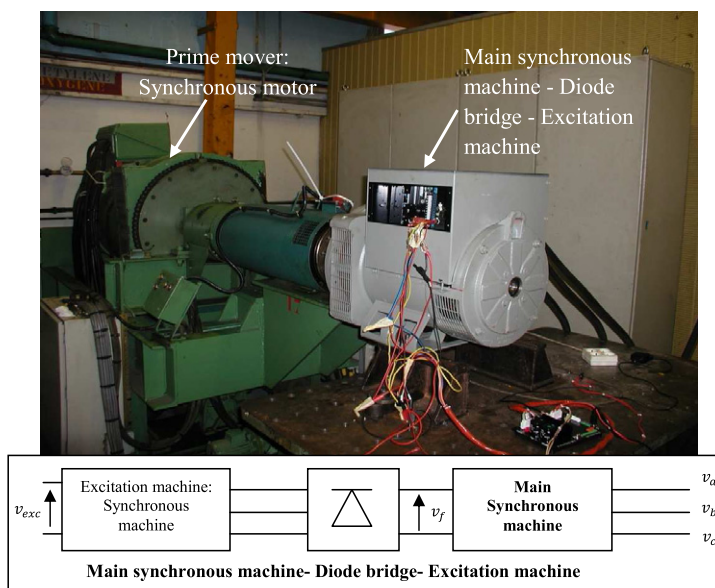| Machine parameters (LSA432L7): 75 kVA						
X_d (Ω)	X_q (Ω)	$\dot{X}_d$ (Ω)	$\ddot{X}_d$ (Ω)	$\ddot{X}_q$ (Ω)	$\dot{T}_{do}$ (ms)	$\dot{T}_d$ (ms)
5.4	2.98	0.218	0.1	0.206	1200	50
$\ddot{T}_d$ (ms)	r_f (Ω)	r_s (Ω)	N_a	N_r	p	
5	1.95	0.135	40	125	2	
Nominal values of the test machine						
Power S_n		75 kVA		Frequency f_n		50 Hz
Voltage U_n		400 V		Speed n_n		1500 tr/min
Current I_n		108 A		Power factor cos (φ)		0.8

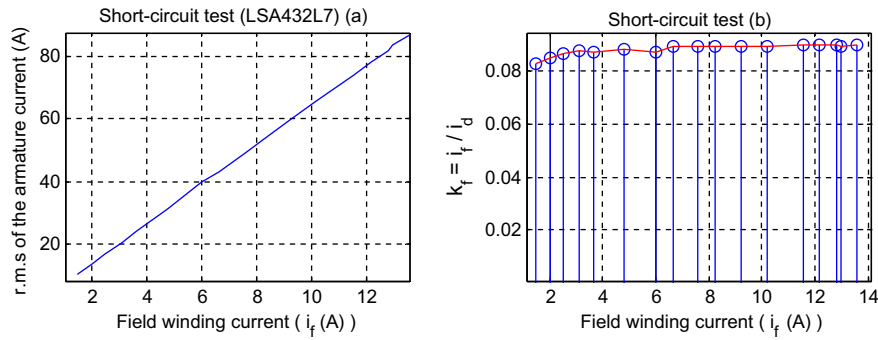**Fig. 5.** Global experimental test bench.

Fig. 6. Short-circuit characteristic and the reduction factor k_f.

In the present work, we have supposed that $k_D = 66$ and $k_Q = 73$. These values are identified in [13] for the synchronous machine (LSA37M6) which has the same technology of the present machine LSA432L7.

4.3. Determination of the machine parameters

By using the obtained value of k_f, the quantities given by the manufacturer (see Table 3) and the relationships given in Table 2, the machine parameters referred to the stator frame can be deduced as shown in Table 4.

k_D and k_Q are used to determine the machine parameters in the natural reference frames. From Eq. (6) the parameters deduced are shown in Table 5.

4.4. Synchronous machine modeling by state equations

In this paper, we have presented two models for a synchronous machine. The first one is presented in the natural reference frames by Eq. (3). This model is rewritten by Eq. (14). The second model is presented by an electrical circuit (see Fig. 4). This circuit contains more information about the structure of the machine (the direct and transverse main inductances, leakage inductances, etc.). By using this model, the influence of any parameter can be easily analyzed.

The software used to simulate the synchronous machine model is Matlab/Simulink. We have simulated the state equations which describe the electrical circuit behavior (Eq. (15)).

The first model (obtained from Eq. (3)):

$$V_d = -r_s i_d + L_q \omega_e i_q - m_{sQ} \omega_e i_Q - L_d \frac{di_d}{dt} + m_{sf} \frac{di_f}{dt} + m_{sD} \frac{di_D}{dt}$$

$$V_q = -r_s i_q - L_d \omega_e i_d + m_{sf} \omega_e i_f - m_{sD} \omega_e i_D - L_q \frac{di_q}{dt} + m_{sQ} \frac{di_Q}{dt}$$

$$V_f = r_f i_f + L_f \frac{di_f}{dt} - m_{sf} \frac{di_d}{dt} + m_{fD} \frac{di_D}{dt} \qquad (14)$$

$$0 = r_D i_D + L_D \frac{di_D}{dt} + m_{fD} \frac{di_f}{dt} - m_{sD} \frac{di_d}{dt}$$

$$0 = r_Q i_Q + L_Q \frac{di_Q}{dt} - m_{sQ} \frac{di_q}{dt}$$

The second model (obtained from Eq. (4)):

Table 4
Parameters of the equivalent circuit in the stator reference frame.

L_{ad} (mH)	L_{aq} (mH)	$L_{\sigma sd}$ (mH)	$L_{\sigma sq}$ (mH)	$\widetilde{L_{\sigma f}}$ (mH)	$\widetilde{L}_{\sigma D}$ (mH)	$\widetilde{L}_{\sigma Q}$ (mH)	$\widetilde{r_D}$ (Ω)	$\widetilde{r_Q}$ (Ω)	$\widetilde{r_f}$ (Ω)
17.07	9.15	0.123	0.334	0.59	0.292	0.334	0.596	1.014	14.71

Table 5
Machine parameters in the natural reference frames.

L_d (mH)	L_q (mH)	L_D (mH)	L_Q (mH)	L_f (mH)	M_{sf} (mH)	M_{sD} (mH)	M_{sQ} (mH)	M_{fD} (mH)	r_f (mΩ)
17.2	9.5	0.0039	0.0018	2280	193.9	0.256	0.125	2.9	1950
r_D (mΩ) = 0.018		r_Q (mΩ) = 0.025							

$$V_d = -r_s i_d + (L_{aq} + L_{\sigma sq})\omega_e i_q - L_{aq}\omega_e \widetilde{i_Q} - (L_{ad} + L_{\sigma sd})\frac{di_d}{dt} + L_{ad}\frac{d\widetilde{i_f}}{dt} + L_{ad}\frac{d\widetilde{i_D}}{dt}$$

$$V_q = -r_s i_d - (L_{ad} + L_{\sigma sd})\omega_e i_d + L_{ad}\omega_e \widetilde{i_f} + L_{ad}\omega_e \widetilde{i_D} - (L_{aq} + L_{\sigma sq})\frac{di_q}{dt} + L_{aq}\frac{d\widetilde{i_Q}}{dt}$$

$$\widetilde{V_f} = \widetilde{r_f}\widetilde{i_f} + \left(L_{ad} + \widetilde{L_{\sigma f}}\right)\frac{d\widetilde{i_f}}{dt} - L_{ad}\frac{di_d}{dt} + L_{ad}\frac{d\widetilde{i_D}}{dt} \qquad (15)$$

$$0 = \widetilde{r_D}\widetilde{i_D} + \left(L_{ad} + \widetilde{L_{\sigma D}}\right)\frac{d\widetilde{i_D}}{dt} + L_{ad}\frac{d\widetilde{i_f}}{dt} - L_{ad}\frac{di_d}{dt}$$

$$0 = \widetilde{r_Q}\widetilde{i_Q} + \left(L_{aq} + \widetilde{L_{\sigma Q}}\right)\frac{d\widetilde{i_Q}}{dt} - L_{aq}\frac{di_q}{dt}$$

The simulation of the machine model developed in the natural reference frames (given by Eq. (14)) and the model in the stator frame (given by Eq. (15)) gives the same results. Therefore, we have chosen to present the implementation and simulation of the second model (Eq. (15)).

4.5. Implementation of the model under Matlab/Simulink

From Eq. (15):

$$\begin{bmatrix} v_d \\ v_q \\ \widetilde{v_f} \\ 0 \\ 0 \end{bmatrix} = Z\begin{bmatrix} i_d \\ i_q \\ \widetilde{i_f} \\ \widetilde{i_D} \\ \widetilde{i_Q} \end{bmatrix} + T\frac{d}{dt}\begin{bmatrix} i_d \\ i_q \\ \widetilde{i_f} \\ \widetilde{i_D} \\ \widetilde{i_Q} \end{bmatrix} \qquad (16)$$

$$Z = \begin{bmatrix} -r_s & L_q\omega_e & 0 & 0 & -L_{aq}\omega_e \\ -L_d\omega_e & -r_s & L_{ad}\omega_e & L_{ad}\omega_e & 0 \\ 0 & 0 & \widetilde{r_f} & 0 & 0 \\ 0 & 0 & 0 & \widetilde{r_D} & 0 \\ 0 & 0 & 0 & 0 & \widetilde{r_Q} \end{bmatrix} \quad T = \begin{bmatrix} -L_d & 0 & L_{ad} & L_{ad} & 0 \\ 0 & -L_q & 0 & 0 & L_{aq} \\ -L_{ad} & 0 & \widetilde{L_f} & L_{ad} & 0 \\ -L_{ad} & 0 & L_{ad} & \widetilde{L_D} & 0 \\ 0 & -L_{aq} & 0 & 0 & \widetilde{L_Q} \end{bmatrix}$$

where:

$$L_d = L_{ad} + L_{\sigma sd}, \quad \widetilde{L_f} = L_{ad} + \widetilde{L_{\sigma f}}, \quad \widetilde{L_Q} = L_{aq} + \widetilde{L_{\sigma Q}}, \quad L_q = L_{aq} + L_{\sigma sq}, \quad \widetilde{L_D} = L_{ad} + \widetilde{L_D} = L_{ad} + \widetilde{L_{\sigma D}}.$$

To simulate the machine model presented by Eq. (16), the concept of state equations under Matlab has been used.
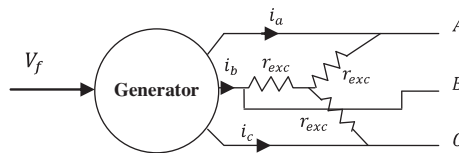

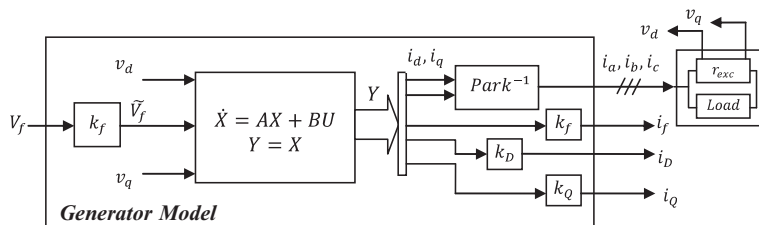Fig. 7. Synchronous generator with infinite outside load.

Fig. 8. Representation of the model under Matlab/Simulink.

$$\dot{X} = AX + BU \quad A = -T^{-1}Z$$
$$Y = X \quad B = T^{-1}$$

(17)

In the modeling of the machine, a star-connected infinite resistance r_{exc} ($10^4\ \Omega$) is putted (see Fig. 7). This allows to generate three-phase voltage and then create terminal *A*, *B*, and *C* on which a three-phase load can be connected. Fig. 8 describes the implementation of this model under Matlab. The particularity of this model that it does not depend on the load; the terminal voltages are measured by using the resistance r_{exc}. The inputs are: v_f, v_d, v_q and the outputs are: i_a, i_b, i_c, i_f, i_D, i_Q.

5. Discussion of results

5.1. Sudden short-circuit

Sudden short-circuit is the sudden application of a three-phase short-circuit across the machine. It represents a high load impact then it is a very useful test to excite the damper windings and measure the subtransient reactances and time constants $\left(\ddot{X}_d, \ddot{T}_d \ldots\right)$ [15].

Fig. 9 shows the phase to phase output voltage obtained by a practical test and by simulation. The short-circuit is done at 53% voltage. Before the sudden short-circuit, the main field winding current obtained by simulation is equal to the measured one. The output voltages obtained by simulation and experimentation have approximately the same waveform (see Fig. 9). The little difference is due to the neglected effects such as the saturation, hysteresis, and harmonics of the main field MMF.

The behavior of a synchronous machine in the sudden short-circuit essentially depends on the subtransient reactance $\ddot{X}_d$, the transient reactance $\dot{X}_d$, the synchronous reactance and also the subtransient time constant $\ddot{T}_d$ and the transient time constant $\dot{T}_d$. By assuming that the magnetizing current is constant during the short-circuit, the armature current flowing during the short-circuit can be approximated as follows [9]:

$$i_a = \left[\frac{V_m}{X+d} + \left(\frac{V_m}{\dot{X}_d} - \frac{V_m}{X_d}\right) \cdot e^{\frac{-t}{\dot{T}_d}} + \left(\frac{V_m}{\ddot{X}_d} - \frac{V_m}{\dot{X}_d}\right) \cdot e^{\frac{-t}{\ddot{T}_d}}\right] \cos(\omega t + \varphi)$$

(18)

where i_a is the instantaneous value of current in phase *a*, V_m is the peak value of the open-circuit voltage prior to the application of the short-circuit, ω is the electrical angular speed of the machine and φ is the phase between the axis of phase a and the direct axis at the instant of short-circuit. Fig. 10 shows the simulated and measured stator *a*-phase current. Fig. 11 shows the simulated and measured main field winding current. From these figures, the machine state before and after the sudden short-circuit is well presented.

Before the short-circuit test, the magnetic state of the machine is determined by the main field winding current because the armature reaction is null. This magnetic state of the machine can be shown by the currents in the main inductances L_{ad} and L_{aq} (see the equivalent circuit Fig. 4). The magnetic state cannot change suddenly. For this reason, at the moment of the short-circuit the main field winding current increases rapidly to compensate the armature reaction which is created by the armature currents.
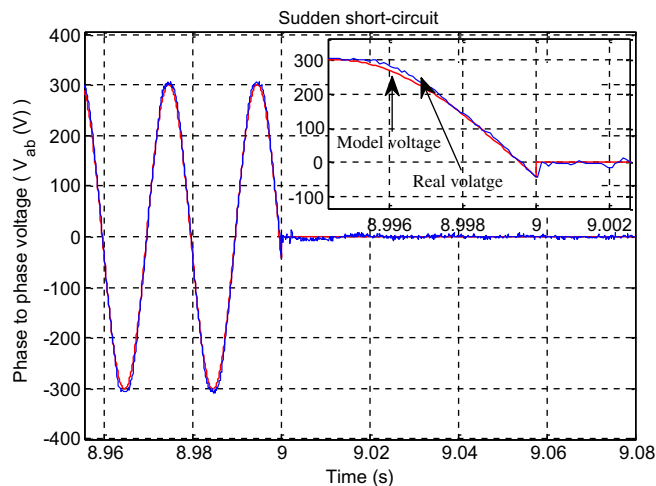

Fig. 9. Calculated and measured phase to phase voltage before the sudden short-circuit.
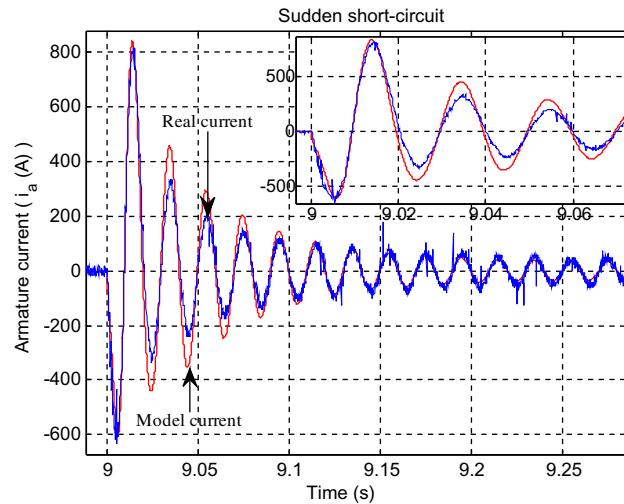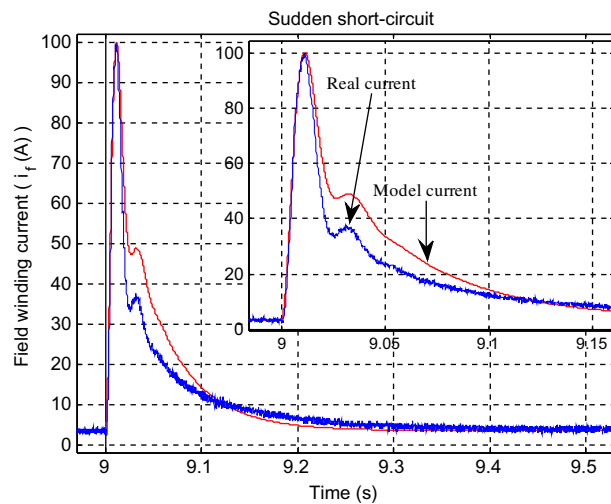
Fig. 10. Model and real armature current.

Fig. 11. Model and real main field winding current.

As shown in Eq. (18), the maximum value reached by the armature currents essentially depends on the peak value of the open-circuit voltage prior to the application of the short-circuit and also to the subtransient reactance $\ddot{X}_d$ and the transient reactance $\dot{X}_d$. For this reason, the calculated and the measured armature current reach 800 A.

As shown in Figs. 10 and 11, in subtransient state, the amplitude of the real armature current decreases more rapidly than the simulated current. The subtransient time constant is defined too long. In transient state, the amplitude of the simulated armature current decreases more rapidly than the real current. The transient time constant is defined too short. This result is well presented in Fig. 11. The convergence between the calculated current and the real current is well shown in steady state.

The discrepancies between simulation and practical results lead to the hypothesis and assumptions that are taken in this paper. Saturation effect and the non-linear nature of the iron portions of the magnetic field circuit are neglected. The quantities given by the manufacturer or measured by using short-circuit test depends on the magnetic state of the machine before the short-circuit test [19]. Before the short-circuit test, the magnetic state of the machine is determined by the main field winding current. In steady state, the magnetic state of the machine becomes too low because of the armature reaction. During the variation of the magnetic state, hysteresis phenomenon is neglected by using a linear model.

The subtransient state depends on the dampers modeling. The representation of the damper behavior by one single inductance is a source of important errors [10]. A third order model which has three damper windings for each axis is the most complex usually employed [17]. It is stated by [20] that it will never be possible to describe the complex behavior of a synchronous machine by a simple lumped parameter network, the number of "virtual" damper windings is chosen accordingly to the required complexity.

The transient state essentially depends on the transient reactance and the transient time constant. Canay inductances are very used to improve the transient state [11], the number of added elements depends on the construction and the type of machine [10].

5.2. Sudden open-circuit

The synchronous machine is short-circuited; suddenly an open-circuit is made. This test is usually used to measure the time constant $\left(\dot{T}_{do}\right)$ and the main field inductance. Fig. 12 shows the model and the real phase to phase output voltage and Fig. 13 shows the model and the real main field winding current before and after the sudden open-circuit. As shown in this figure, there is a very good agreement with practical results. The real main field winding current and the calculated current have very similar shape. The difference in the value of the current peak comes from the damper modeling. The convergence between the real field winding current and the calculated current is well shown in transient state and steady state. In sub-transient state, there is no effect of the armature currents. In transient state, the influence of the damper currents is too low because the armature currents are null. For this reason, by neglecting the influence of the damper windings, this test is usually used to measure the main field winding inductance.
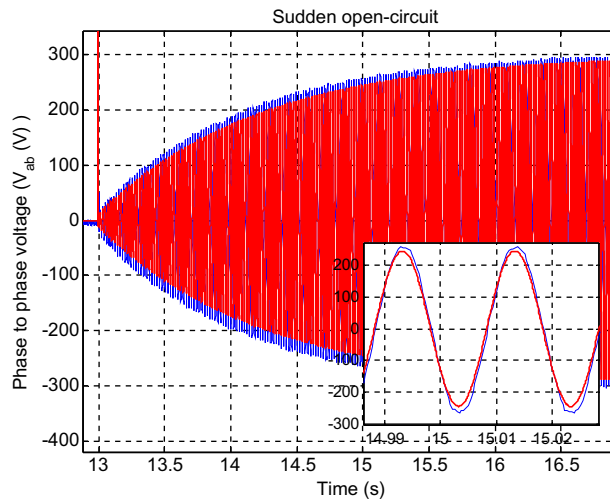

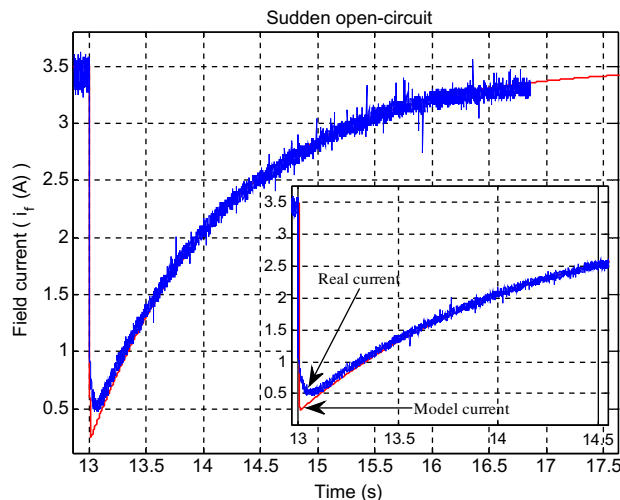Fig. 12. Model and real phase to phase voltage.

Fig. 13. Model and real main field winding current.

Table 6
Calculation of the model fitness.

BFT	i_f	i_a	V_{ab}
Sudden short-circuit	BFT = 70.3%	BFT = 75.3%	
Sudden open-circuit	BFT = 94.1%		BFT = 94.2%

5.3. Measure of the model fitness

The fitness of the model can be measured by using the best fit percentage (BFT) [21,22] defined as follows:

$$\text{BFT}_\% = 100 \cdot \left(1 - \frac{\|y_e - y\|_2}{\|y - \bar{y}\|_2} \right)$$

where:

$y = (y_1, y_2, \ldots, y_N)$ is the measured output.
$y_e = (y_{e1}, y_{e2}, \ldots, y_{eN})$ is the output of the model.

$\bar{y}$ is the mean value of the measured output.

$$\|y_e - y\|_2 = \sqrt{\sum_{i=1}^{N}(y_e - y)^2} \quad \text{and} \quad \|y - \bar{y}\|_2 = \sqrt{\sum_{i=1}^{N}(y - \bar{y})^2}$$

where N is the number of samples used to calculate the BFT.

The tests done in this paper provide two outputs for each one. For the sudden short-circuit, the outputs are the main field winding current (i_f) and the armature current (i_a) (see Figs. 10 and 11). For the sudden open-circuit, the outputs are the main field winding current (i_f) and the phase to phase output voltage (V_{ab}) (see Figs. 12 and 13). Table 6 presents the BFT value for each output.

The BFT is calculated during the subtransient and transient state of each test. In sudden short-circuit case, the steady state is established after 0.3 s of doing the short-circuit. The used sampling interval is 2.5 ms. In sudden open-circuit, the steady state is established after 3.5 s. The used sampling interval is 25 ms.

The results given in Table 6 highlight the discussion given in Sections 5.1 and 5.3. In addition of the above discussion, the measuring instruments add some errors because of the limited bandwidth of these instruments.

6. Conclusion

This paper presents a complete procedure to determine a synchronous machine model by taking into account the existence of damper windings. The particularity of this work is the analysis of the equivalent circuit in the (d,q) natural reference frames and in the (d,q) stator reference frame. Three methods are presented to compute the main field reduction factor. Two other methods are proposed to compute this factor without any requirement of design information. This paper also proves that a 'bad choice' of the reduction factors for the d-axis and q-axis damper windings does not affect the terminal behavior of the machine. The implementation of the model using Matlab/Simulink is done by using an external high value resistance which allows creating terminals on the model. Therefore, a sudden short-circuit test or a sudden open-circuit test can be achieved without the modifying the proper structure of the model. By making a sudden open-circuit, a very good agreement between simulation and practical results is noticed. With a sudden short-circuit, the dampers are excited and there are some discrepancies between simulation and practical results. These discrepancies are essentially related to the hypothesis and assumptions that are taken about the damper modeling, saturation and hysteresis phenomena.

Acknowledgements

References

[1] S. Racewicz, D. Riu, N. Retière, P. Chzran, Non-linear half-order modeling of synchronous machine, in: International Electrical Machines and Drives Conference IEMDC, Miami, United States, 2009.
[2] A. Kumar, S. Marwaha, A. Singh, A. Marwaha, Performance investigation of a permanent magnet generator, Simulation Modelling Practice and Theory 17 (2009) 1548–1554.
[3] S. Maiti, C. Chakraborty, S. Sengupta, Simulation studies on model reference adaptive controller based speed estimation technique for the vector controlled permanent magnet synchronous motor drive, Simulation Modelling Practice and Theory 17 (2009) 585–596.
[4] S. Giurgea, H.S. Zire, A. Miraoui, Two-stage surrogate model for finite element-based optimization of permanent-magnet synchronous motor, circuits, IEEE Transaction on Magnetics 43 (49) (2007) 3607–3613.

 [5] G. Cupta, S. Marwaha, M.S. Manna, Finite element method as an aid to machine design: a computational tool, in: Proceedings of the COMSOL, Conference, Bangalore, 2009.
 [6] E. Mouni, S. Tnani, G. Champenois, Synchronous generator output voltage real-time feedback control via Hinfini strategy, IEEE Transactions on Energy Conversion 24 (6) (2008) 678–689.
 [7] G. Grater, T. Doyle, Propulsion powered electric guns – a comparison of power system architectures, IEEE Transaction on Magnetics 29 (1993) 963–968.
 [8] S.K. Sahoo, G.T.R. Das, V. Subrahmanyam, Implementation and simulation of direct torque control scheme with the use of FPGA circuit, ARPN Journal of Engineering and Applied Sciences 3 (2) (2008).
 [9] E. Mouni, S. Tnani, G. Champenois, Synchronous generator modelling and parameters estimation using least squares method, Simulation Modelling Practice and Theory, vol. 16/6, Elsevier, Amsterdam, 2008. pp. 678–689.
[10] J. Verbeeck, R. Pintelon, P. Lataire, standstill frequency response measurement and identification methods for synchronous machines, Ph.D. Thesis at Vrije universiteit Brussel, Belgium, 2000.
[11] H. Radjeai, R. Abdessemed, S. Tnani, A Method to improve the Synchronous Machines Equivalent circuits, in: International Conference on "Computer as Tools", September 2007.
[12] M. Kostenko, L. Piotrovski, Machines électriques, Techniques Soviétique, 1965.
[13] S. Lasquellec, M.F. Benkhoris, M. Féliachi, A saturated synchronous machine study for the converter-machine-command set simulation, Journal of Physics III France 7 (1997) 2239–2249.
[14] J. Verbeeck, R. Pintelon, P. Lataire, Relationships between parameters sets of equivalent synchronous machine models, IEEE Transactions on Energy Conversion 14 (4) (1999).
[15] IEC 60034-4 Ed.3, Rotating electrical machines. Part 4: methods for determining synchronous machine quantities from tests, in: International Electrotechnical Commission, May 2008.
[16] A. Kapun, M. Čurkovič, A. Hace, K. Jezernik, Identifying dynamic model parameters of a BLDC motor, Simulation Modelling Practice and Theory 16 (2008) 1254–1265.
[17] R. Gordon, S. Awad, M. Awad, On equivalent circuit modeling for synchronous machines, IEEE Transactions on Energy Conversion 14 (4) (1999).
[18] M. Calvo, O.P. Malik, Synchronous machines parameter estimation using artificial neural networks, Ph.D. Thesis at Calgary University, Alberta, Canada, April 2000.
[19] H. Rehaoulia, H. Henao, G.A. Capolino, Modeling of synchronous machines with magnetic saturation, Electric Power Systems Research 77 (5–6) (2007) 652–659.
[20] M.A. Arjona, D.C. MacDonald, Characterizing the d-axis machine model of a turbogenerator using finite elements, IEEE Transactions on Energy Conversion 14 (3) (1999) 340–346.
[21] R. Tóth, P.M.J. Van den Hof, P.S.C. Heuberger, Modeling and identification of linear parameter-varying systems, an orthonormal basis function approach, Thesis at University of Pannonia, December 2008.
[22] L. Ljung, System Identification Toolbox for Use with Matlab, The Mathworks Inc., 2006.